

# Particle Pinch Model of Passing/Trapped High-Z Impurity with Centrifugal Force Effect<sup>\*</sup>)

Yusuke SHIMIZU, Takaaki FUJITA, Atsushi OKAMOTO, Hideki ARIMOTO, Nobuhiko HAYASHI<sup>1)</sup>, Kazuo HOSHINO<sup>2)</sup>, Tomohide NAKANO<sup>1)</sup> and Mitsuru HONDA<sup>1)</sup>

*Nagoya University, Furo-cho, Chikusa-ku, Nagoya 464-8603, Japan*

<sup>1,\*\*)</sup>*Japan Atomic Energy Agency, 801-1 Mukoyama, Naka 311-0193, Japan*

<sup>2,\*\*)</sup>*Japan Atomic Energy Agency, 2-166 Omotedate, Obuchi, Rokkasho 039-3212, Japan*

(Received 30 November 2015 / Accepted 24 March 2016)

The inward pinch model for high-Z impurity ions in a toroidally rotating plasma has been improved to take account of trapped particles and the centrifugal force effect. It is found that the PHZ pinch is large for the barely trapped particles and the pinch velocity increases with the rotation velocity as in the original model.

© 2016 The Japan Society of Plasma Science and Nuclear Fusion Research

Keywords: tungsten accumulation, toroidal rotation, PHZ pinch, centrifugal force

DOI: 10.1585/pfr.11.2403082

## 1. Introduction

In JT-60U, it was observed that tungsten accumulation was enhanced with increase in the toroidal rotation in the opposite direction (CTR-rotation) to the plasma current in H-mode plasmas [1]. From theoretical considerations, Hoshino *et al.* proposed the PHZ (inward Pinch of High-Z impurity due to the atomic process) pinch model and the Er pinch model, both of which are related to the toroidal rotation and the radial electric field [2]. We introduced these pinch models in TOTAL code and studied dependence of the tungsten accumulation on the toroidal rotation [3]. We investigated the effect of the PHZ pinch only because the Er pinch model equation was not valid in the experimental conditions analyzed. The larger accumulation observed experimentally at the higher toroidal rotation was reproduced in simulation with the PHZ pinch. However, the dependence on the toroidal rotation was weaker in the simulations than in the experiments.

In the experiment, the toroidal rotation velocity of tungsten ions is determined by collisions with the bulk ions (drag force) and hence the bulk plasma and the tungsten ions rotate with the similar speed. In the original PHZ pinch model, however, the orbit of tungsten ions was analyzed neglecting the effect of bulk plasma rotation on the particle orbit. In addition, the tungsten ion velocity vector was assumed to be parallel to the magnetic field focusing on the case that the Mach number for tungsten ions is larger than unity. The plasma rotation causes the centrifugal force, which makes poloidal asymmetry in the heavy impurity ion density as observed in JET [4]. In this study,

we generalize the PHZ model for the ions with the arbitrary pitch angle and then calculate the tungsten ion orbit including the centrifugal force taking into account of the effects of the plasma rotation. In section 2, the mechanism of the original model is reviewed. The PHZ pinch model including the trapped particle is presented in section 3. Section 4 gives development of the revised PHZ pinch with the plasma rotation effect and the results of the revised model. Section 5 gives summary and future plan.

## 2. Original PHZ Pinch Model

The PHZ pinch is caused by change in the ion charge state along its collisionless drift orbit. In the original model, the orbit of tungsten ions is analyzed in a stationary plasma neglecting the effect of plasma rotation on the particle orbit.

High-Z impurity ions are accelerated up to the toroidal rotation velocity of the background plasma by friction. Because the high-Z impurity ions are relatively massive, their kinetic energy becomes large and then their drift orbit deviates largely from the magnetic surface. The charge state  $Z$  varies as the electron temperature  $T$  changes along the drift orbit. The magnetic drift velocity also varies along the orbit since it is in inverse proportion to  $Z$ . If the poloidal rotation period approximates the characteristic time of the ionization / recombination, the variation of the charge state and the magnetic drift velocity is delayed due to the time needed for the ionization / recombination processes. This delay of the magnetic drift velocity variation causes an inward pinch called PHZ pinch.

The PHZ pinch velocity is given by the following equation [2];

$$V_{\text{PHZ}} = \frac{v_{d0}^2}{2Z_0} \frac{C_T C_{\nabla T}}{C_Z^2 + \omega^2}, \quad (1)$$

author's e-mail: fujita@ees.nagoya-u.ac.jp

<sup>\*</sup>) This article is based on the presentation at the 25th International Toki Conference (ITC25).

<sup>\*\*)</sup> The current affiliation is National Institutes for Quantum and Radiological Science and Technology.

where  $Z_0$  is the charge number of the impurity ion in the ionization equilibrium at the temperature on the flux surface,  $v_{d0}$  is the magnetic drift velocity of the impurity ion with charge state  $Z_0$ ;  $v_{d0} = mV_t^2/Z_0eRB$ ,  $\omega$  is the angular frequency of the poloidal motion of impurity ion;  $\omega = (V_t - E_r/B_\theta)/(qR_0)$ ,  $V_t$  is the toroidal rotation velocity of the tungsten ion,  $B_\theta$  is poloidal magnetic field,  $C_T = n_e\partial(\gamma_k - \alpha_k)/\partial T$ ,  $C_Z = n_e\partial(\gamma_k - \alpha_k)/\partial Z$  and  $C_{\nabla T} = dT/dr$ ;  $\gamma_k$  is the ionization rate and  $\alpha_k$  is the recombination rate.

### 3. PHZ Pinch for Arbitrary Pitch Angle

In the original model, it was assumed that  $V_t \gg v_{th}$  and so the spread of particle velocity due to the thermal velocity  $v_{th}$  was ignored. We consider the PHZ pinch for arbitrary pitch angle including the trapped particle. The radial electric field is not considered in this section.

The orbit is illustrated for trapped particles in Fig. 1. Writing the major radius coordinate  $R = R_0 + r \cos \theta$ , the magnetic field is given by,

$$B = \frac{R_0 B_0}{R} = \frac{B_0}{1 + (r/R_0) \cos \theta}. \quad (2)$$

The kinetic energy  $E = mv^2/2$  and the magnetic moment  $\mu = mv_\perp^2/(2B)$  are conserved

$$v^2 = v_{\parallel 0}^2 + v_{\perp 0}^2 = v_{\parallel}^2 + v_{\perp}^2, \\ \frac{v_{\perp}^2}{B} = \frac{v_{\perp 0}^2}{B_{\min}},$$

where  $v$  is the particle velocity,  $v_{\parallel}$  and  $v_{\perp}$  are the velocity parallel and perpendicular to the magnetic field, respectively. The subscript 0 represents the values where the magnetic field has the minimum value  $B_{\min}$ . The pitch angle parameter  $\xi$  is given by  $\xi = v_{\parallel 0}/v$ . The parallel velocity is derived from the conservation of the kinetic energy and the magnetic moment:

$$\frac{dv_{\parallel}}{dt} = -\frac{r \sin \theta \mu B_0}{qR^2 m_z}. \quad (3)$$

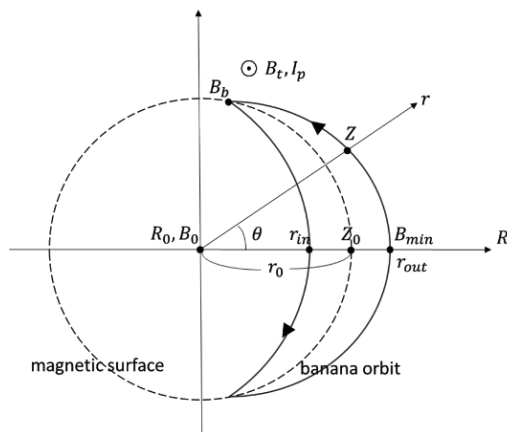


Fig. 1 Schematic diagram for trapped particles.

The charge state  $Z$ , the minor radius  $r$  and the poloidal angle  $\theta$  are given by

$$\frac{dZ}{dt} = C_T C_{\nabla T} (r - r_0) + C_Z (Z - Z_0), \quad (4)$$

$$\frac{dr}{dt} = v_r = -v_d \sin \theta, \quad (5)$$

$$\frac{d\theta}{dt} = \frac{v_{\parallel}}{qR_0}, \quad (6)$$

where  $v_d$  is the local drift velocity;  $v_d = m(v_{\parallel}^2 + v_{\perp}^2/2)/ZeR_0B_0$ . A new code has been developed for solving these equations. The orbit of tungsten ion is calculated with the 4th order Runge-Kutta method using eqs. (5) and (6) neglecting the variation of  $Z$  along the orbit. For the orbit thus obtained, the change of  $Z$  is calculated using eq. (4). This two-step procedure is basically the same as that employed in the original analytical PHZ model [2]. The PHZ pinch velocity is then given by

$$V_{\text{PHZ}} = \langle v_r \rangle = \frac{1}{T} \int_0^T v_r dt, \quad (7)$$

where  $T$  is the period for completing the orbit in the poloidal crosssection.

Figure 2 shows the comparison between the results of the newly developed code and the original analytic model for the case with  $\xi = \pm 1$ . The JT-60U like parameters as shown in Table 1 are assumed. At  $T = 1500$  eV,  $Z_0 = 34$ ,  $C_T = 8.01$  eV $^{-1}$  s $^{-1}$  and  $C_Z = -512$  s $^{-1}$  are obtained for the tungsten ion. As shown in Fig. 2, the results of the code agree with the analytic model and we have verified the developed code for calculating the PHZ pinch velocity.

Figure 3 shows the banana width for trapped particles or the deviation from the magnetic surface for passing particles, and the  $V_{\text{PHZ}}$  as function of  $\xi$  for 3 cases of  $v$ . The

Table 1 Plasma parameters for evaluation.

$R_0$	3.4 m
$r_0$	0.8 m
$B_0$	3.5 T
$n_e$	$2 \times 10^{19}$ m $^{-3}$
$T_e$	1500 eV
$C_{\nabla T}$	$-5000$ eV m $^{-1}$

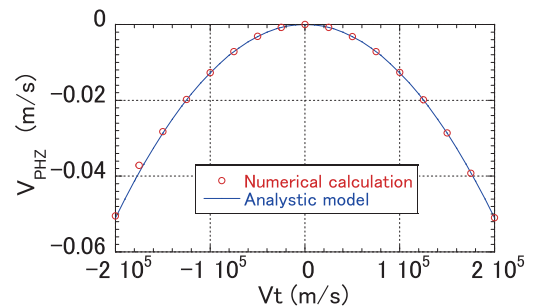


Fig. 2 Comparison between the results of the developed code and the analytic model.

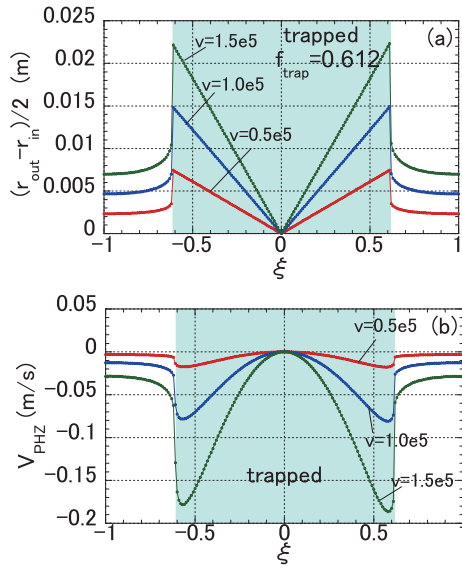


Fig. 3 (a) The banana width or deviation from the magnetic surface and (b)  $V_{\text{PHZ}}$  as a function of the pitch angle parameter  $\xi$  for  $v = 0.5 \times 10^5$  m/s,  $v = 1 \times 10^5$  m/s and  $v = 1.5 \times 10^5$  m/s.

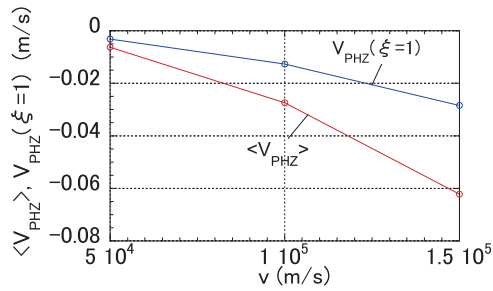


Fig. 4 Comparison between  $\langle V_{\text{PHZ}} \rangle$  and  $V_{\text{PHZ}}(\xi = 1)$  or the original model.

banana width is large around banana boundary or for the barely trapped particles and it increases with increase in the  $v$ . The particles with  $\xi$  in the hatched regions draw the banana orbit in the calculation. The fraction of banana particles  $f_{\text{trap}}$  is almost consistent with the theoretical value given by the following equation.

$$f_{\text{trap}} = \sqrt{1 - \frac{R_0 - r_0}{R_0 + r_0}}.$$

The  $V_{\text{PHZ}}$  is also large around the banana boundary since change in the charge state  $Z$  becomes larger with increase in the radial displacement of the particle orbit.

From Fig. 3, it is expected that the  $V_{\text{PHZ}}$  becomes larger when the spread of particle velocity due to the thermal velocity is taken into account. The average PHZ pinch velocity  $\langle V_{\text{PHZ}} \rangle$  for the isotropic velocity distribution was evaluated by averaging  $V_{\text{PHZ}}$  for  $\xi$ . As shown in Fig. 4,  $\langle V_{\text{PHZ}} \rangle$  is higher than the  $V_{\text{PHZ}}(\xi = 1)$  which corresponds to the original PHZ model.

## 4. PHZ Pinch with the Centrifugal Force Effect

### 4.1 Mechanism

In a rotating plasma, tungsten ions are concentrated on the low field side of the magnetic surface due to the centrifugal force [4]. Thereby the fraction of the trapped impurity particles increases. Here the orbit of tungsten ions in a rotating plasma is analyzed using the frame rotating with the same speed as the plasma. It is considered that the tungsten ions and the bulk plasma rotate at the similar velocity. Then, in the rotating frame, tungsten ions move only at the thermal speed ( $v_{\text{th},z} = \sqrt{2kT_i/m_w}$ ) and hence the velocity is smaller than in the original model when the Mach number is larger than unity. In this study, the radial electric field  $E_r$  is not considered as the first step. Note that this means that  $E_r$  is zero in the rotating frame and then it is finite in the laboratory frame (positive  $E_r$  in the CO rotating plasma).

In the rotating frame, the sum of the potential energy derived from the centrifugal force and the kinetic energy,  $\varepsilon$  in eq. (8), is conserved [5, 6]

$$\varepsilon = \frac{1}{2}m_Z(v^2 - R^2\Omega_*^2), \quad (8)$$

$$\Omega_* = \Omega \left[ 1 - \frac{Zm_i T_e}{m_Z(T_i + T_e)} \right]^{1/2}, \quad (9)$$

where  $\Omega$  is the angular frequency of the plasma rotation;  $\Omega = V_t/R_0$ ,  $m_i$  and  $m_Z$  denote the bulk and impurity ion mass, respectively. Since  $I_p$  and  $B_t$  are in the negative direction of the toroidal angle as shown Fig. 1, the CTR plasma rotation corresponds to  $V_t > 0$  and the CO plasma rotation to  $V_t < 0$ . The magnetic moment  $\mu$  is also conserved in the rotating frame, as it is in the laboratory frame. The initial particle speed in the orbit calculation is adjusted so that the speed corresponding to the average kinetic energy in the orbit is equal to the thermal speed on the flux surface. The centrifugal force affects both of the drift velocity and the parallel velocity.

The drift velocity is given by

$$v_d = \frac{m}{ZeR_0B_0} \left[ \left( v_{\parallel}^2 + \frac{v_{\perp}^2}{2} \right) + \Omega_*^2 R^2 + 2v_{\parallel}\Omega R \right]. \quad (10)$$

The second term and the third term on the right-hand side come from the centrifugal force and the Coriolis force, respectively [5]. Since the definition of the coordinate system is different from that in [5], we modified the sign of the Coriolis force from minus to plus in Eq. (10). The evolution of  $v_{\parallel}$  is given as follows. By differentiating eq. (8), we have

$$v_{\parallel} \frac{dv_{\parallel}}{dt} = -\frac{\mu}{m} \frac{dB}{dt} + \Omega_*^2 R \frac{dR}{dt}, \quad (11)$$

where the conservation of the magnetic moment

$$v_{\perp} \frac{dv_{\perp}}{dt} = \frac{\mu}{m} \frac{dB}{dt}, \quad (12)$$

is employed. Since we do not consider the radial electric field, the drift velocity is in the  $Z$  direction and then there

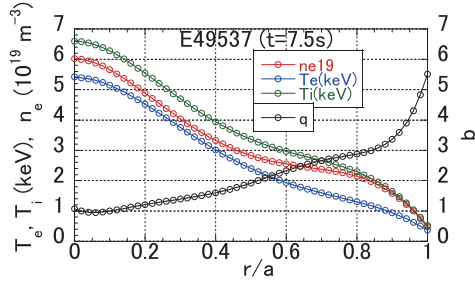


Fig. 5 Radial profiles of plasma parameters of the experimental data used in the calculation.

is no change in  $R$  or in  $B$  due to the drift velocity, Thus we find

$$\frac{d}{dt} = v_{\parallel} \frac{d}{dl} = v_{\parallel} \frac{B_{\theta}}{rB_0} \frac{d}{d\theta} = \frac{v_{\parallel}}{qR_0} \frac{d}{d\theta}, \quad (13)$$

in the right hand side of eq. (11). Substituting eq. (13) into eq. (11), we obtain

$$v_{\parallel} \frac{dv_{\parallel}}{dt} = -\frac{v_{\parallel}}{qR_0} \left( \frac{\mu}{m} \frac{dB}{d\theta} - \Omega_*^2 R \frac{dR}{d\theta} \right). \quad (14)$$

Hered  $dR/d\theta = -r \sin \theta$  while  $dB/d\theta$  is obtained by differentiating eq. (2),

$$\frac{dB}{d\theta} = \frac{B_0 R_0}{R^2} r \sin \theta. \quad (15)$$

Then, substituting them into eq. (14) we finally find

$$\frac{dv_{\parallel}}{dt} = -\frac{r \sin \theta}{qR^2} \left( \frac{\mu B_0}{m_z} + \Omega_*^2 \frac{R^3}{R_0} \right). \quad (16)$$

When there is no rotation ( $\Omega_* = 0$ ), eq. (16) agrees with eq. (3). The orbit of tungsten ion is calculated with eqs. (5) and (6), using the  $v_d$  and  $v_{\parallel}$  obtained by eqs. (10) and (16). The subsequent procedure is the same as that described in section 3.

## 4.2 Conditions

The plasma parameters are as follows: the plasma major radius  $R_0 = 3.35$  m, the magnetic field  $B_0 = 3.5$  T, the plasma current = 1.6 MA, the neutral beam (NB) heating power = 15 MW.  $T_e$ ,  $T_i$ ,  $n_e$  and  $q$  are taken from experimental data, shot E049537 ( $t = 7.5$  s) as shown in Fig. 5. Other parameters are shown in Table 2. The ionization rate  $\gamma_k$  and the recombination rate  $\alpha_k$  of the tungsten ions are taken from [7], and  $C_T$  and  $C_Z$  are calculated with experimental density and temperature profiles.

## 4.3 Results

Figure 6 shows  $V_{PHZ}$  as a function of  $\xi$  and  $\langle V_{PHZ} \rangle$  and  $f_{trap}$  at  $r/a = 0.76$  as a function of  $V_t$ . The  $V_{PHZ}$  becomes larger with increase in the rotation velocity. The fraction of trapped particles also becomes larger with increase in the rotating velocity, which results in increase in  $\langle V_{PHZ} \rangle$ . When the rotation velocity is doubled,  $\langle V_{PHZ} \rangle$  is also almost doubled.

Table 2 Plasma parameters in the JT-60U experiment used for the analysis.

$r/a$	0.76	0.4
$v_{th,w}$	$4.58 \times 10^4$ m/s	$6.25 \times 10^4$ m/s
$Z_0$	30	41
$C_{VT}$	$-2217$ eV m <sup>-1</sup>	$-6770$ eV m <sup>-1</sup>
$C_T$	$2.78$ eV <sup>-1</sup> s <sup>-1</sup>	$16.1$ eV <sup>-1</sup> s <sup>-1</sup>
$C_Z$	$-1494$ s <sup>-1</sup>	$-512$ s <sup>-1</sup>

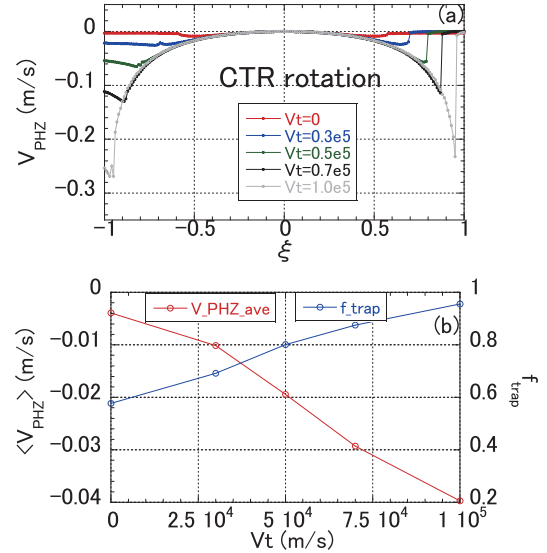


Fig. 6 (a)  $V_{PHZ}$  as a function of  $\xi$  and (b)  $\langle V_{PHZ} \rangle$  and  $f_{trap}$  as functions of  $V_t$  for  $r/a = 0.76$ .

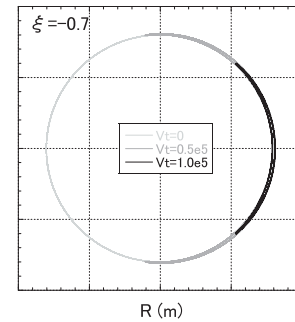


Fig. 7 The particle orbit for particle with  $\xi = 0.7$ . Particles are concentrated on the low field side by the centrifugal force with increase in the toroidal rotation velocity.

As shown in Fig. 7, passing particles have become trapped particles by the effect of centrifugal force with increase in the toroidal rotation velocity.

The asymmetry in  $V_{PHZ}$  with respect to  $\xi$ , as seen in Fig. 6(a) for the large rotation velocity, is caused by the Coriolis force. As shown in Fig. 8,  $V_{PHZ}$  is symmetrical for the CTR rotation and for the CO rotation. Note that the particles with  $\xi = 1$  rotate with a higher speed than the plasma in the CO rotating plasma while it rotates with a

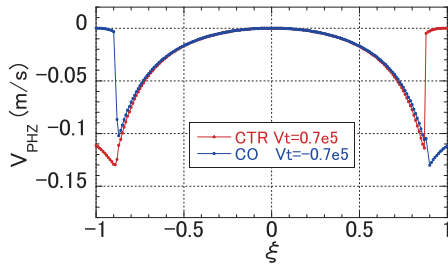


Fig. 8 Comparison with CTR rotation and CO rotation at  $V_t = 0.7 \times 10^5$  m/s for example.

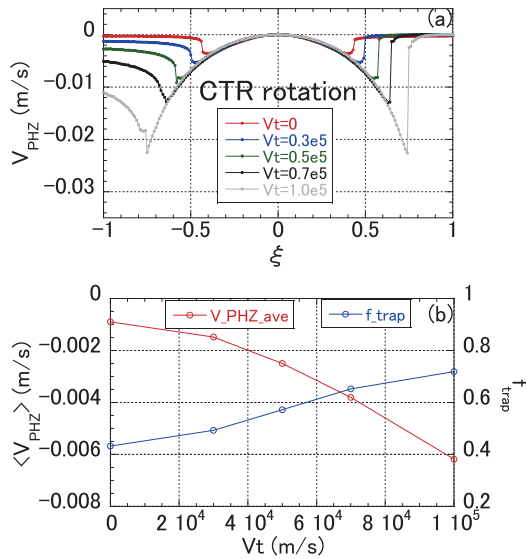


Fig. 9 (a)  $V_{\text{PHZ}}$  as a function of  $\xi$  and (b)  $\langle V_{\text{PHZ}} \rangle$  and  $f_{\text{trap}}$  as functions of  $V_t$  for  $r/a = 0.4$ .

smaller speed or towards the opposite direction in the CTR rotating plasma.

Figure 9 shows the results for  $r/a = 0.4$ . It represents the same characteristics as those for  $r/a = 0.76$ . Because of difference in the coefficient such as  $C_T$  and  $C_Z$ , the value of  $\langle V_{\text{PHZ}} \rangle$  is smaller than that for  $r/a = 0.76$ .

## 5. Summary

We developed a revised PHZ pinch model taking into account of the distribution of the particle pitch angle and the effect of bulk plasma rotation on the particle orbit. The PHZ pinch is large for the barely trapped particles. It was found that  $V_{\text{PHZ}}$  increased with increase in the rotation velocity as in the original model.

In this study we did not consider the radial electric field  $E_r$ . In future work, we plan to extend the newly developed PHZ pinch model to include  $E_r$ .

## Acknowledgments

This study was carried out under the National Centralized Tokamak Collaborative Research Program in JAEA. This study was supported by JSPS KAKENHI Grant Number 25420895.

- [1] T. Nakano, *J. Nucl. Mater.* **415**, S327 (2011).
- [2] K. Hoshino *et al.*, *Nucl. Fusion* **51**, 083027 (2011).
- [3] Y. Shimizu *et al.*, *Plasma Fusion Res.* **10**, 3403062 (2015).
- [4] C. Angioni *et al.*, *Nucl. Fusion* **54**, 083028 (2014).
- [5] K.L. Wong *et al.*, *Phys. Fluids B* **1**, 545 (1989).
- [6] K.G. McClements *et al.*, *Plasma phys. Control. Fusion* **51**, 115009 (2009).
- [7] OPEN-ADAS, <http://open.adas.ac.uk/>